

New color-magnitude diagram for the open cluster IC 4651

Deep Strömrgren *uvby* CCD photometry in a large field^{*,**}

S. Meibom^{1,2}

¹ Niels Bohr Institute for Astronomy, Physics, and Geophysics, Astronomical Observatory, Juliane Maries Vej 30, 2100 Copenhagen, Denmark

² Astronomy Department, University of Wisconsin, Madison, WI-53706, USA (meibom@astro.wisc.edu)

Received 20 March 2000 / Accepted 26 July 2000

Abstract. New accurate CCD photometry in the *u*, *v*, *b* and *y* bands of the Strömrgren system filters has been obtained for 17640 stars to $V \sim 20^m$ in a $\sim 21' \times 21'$ field centered on the intermediate-age open cluster IC 4651. The resulting color-magnitude diagram (CMD) is substantially improved in completeness and accuracy compared to previous studies of IC 4651.

Specifically, this study has: 1) more than doubled the known size of the cluster area on the sky, 2) more than doubled the number of stars brighter than $V \sim 14^m$, 3) added 160 “new” candidate member stars to the turn-off region of the CMD, 4) identified ~ 600 fainter stars that trace a previously undetected and well-defined main-sequence down to $V \sim 18^m$, and 5) enabled a very accurate determination of true distance modulus ($(m - M)_0 = 10.03 \pm 0.1$) by fitting the Hyades main-sequence over the long stretch of the cluster main-sequence. The $(v - y) - V$ CMD defines the main-sequence significantly better than the traditional $(b - y)$ or $(B - V)$ CMDs. These findings make IC 4651 a perfect target for testing stellar evolution models.

A correlation is found between the CMD and the radial distance of the stars to the cluster center. The fainter main-sequence stars are less centrally concentrated, as predicted by theory. Overall, IC 4651 appears to be a moderately dynamically evolved cluster ideally suited for testing of dynamical models.

Key words: Galaxy: open clusters and associations: individual: IC 4651 – stars: Hertzsprung–Russel (HR) and C-M diagrams

1. Introduction

Observations of star clusters have led to substantial progress in such areas of Galactic astrophysics as, e.g. the formation and evolution of the Milky Way (Gilmore et al. 1990), determination of distances, ages, and chemical compositions of sub-populations in our Galaxy (Friel 1995; Gilmore et al. 1990), and empirical testing of stellar evolution models (Vandenberg

* Based on observations obtained with the Danish 1.5-m telescope at the European Southern Observatory, La Silla, Chile.

** Tables 1, 2 and 3 are only available in electronic form at the CDS via anonymous ftp to cdsarc.u-strasbg.fr (130.79.128.5) or via <http://cdsweb.u-strasbg.fr/Abstract.html>

1983, 1985; Carraro et al. 1993; Demarque et al. 1994). Theoretical models and numerical simulations of stellar and dynamical evolution in open clusters have reached a level where high-quality observations have become essential for meaningful comparisons to be carried out (Spitzer & Mathieu 1980; de la Fuente Marcos 1997 and references therein).

However, observational shortcomings such as limited field-size and faint magnitude limit, imprecise broad-band photometry, uncertain membership assignment, and incomplete identification of cluster binaries, still impede more detailed comparisons with model results. A striking example of the importance of these effects has recently been discussed by Nordström et al. 1997.

Here we report a new, substantially improved CMD for the fairly rich intermediate age southern open cluster IC 4651 ($\alpha_{2000} = 17^h 24^m 47^s$; $\delta_{2000} = -49^\circ 56' 57''$ and $l = 340^\circ 07'$, $b = -7^\circ 88'$). A detailed analysis of the stellar content, age, and dynamical evolution of this cluster will be published separately, based on the photometry presented here and new extensive radial-velocity results.

2. Recent studies of IC 4651

A sizeable literature on IC 4651 already exists, including the photometric studies by Eggen 1971 (photoelectric *UBV* photometry of 102 stars; field $\sim 10' \times 10'$); Lindoff 1972 (photographic *UBV* photometry of 291 stars; field radius $\sim 7'$); Smith 1982 (DDO photometry of 14 stars); Anthony-Twarog & Twarog 1987 (CCD *uvby*- H_β photometry of 134 stars; two fields of $\sim 3' \times 5'$); Anthony-Twarog et al. 1988 (CCD *BV* photometry of 113 stars; field $\sim 3' \times 5'$ + photographic *BV* photometry of 178 stars; field radius $\sim 4.7'$); Nissen 1988 (photoelectric *uvby*- H_β photometry of 10 stars); Eggen 1989 (*by* and *RI* photometry for 17 stars); and Kjeldsen & Frandsen 1991 (CCD *UBV* photometry for 165 stars). Mermilliod et al. (1995) presented radial-velocity observations of red giants, and evolutionary models for the stars in IC 4651 were discussed by Mazzei & Pigatto 1988, Bertelli et al. 1992, and Meynet et al. 1993.

The studies mentioned above suggest the following properties for IC 4651: True distance modulus from $(m - M)_0 = 9.40$

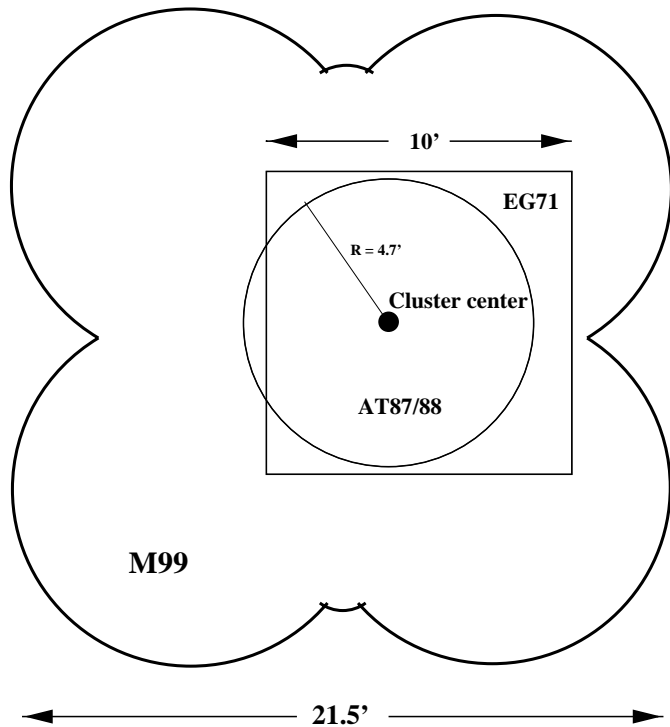


Fig. 1. Outline of the field around IC 4651 observed in the present study (M99). The curved shape is due to cutoff of the vignettted areas caused by the circular Strömrgren filters. The fields observed by Eggen (1971) (EG71), Anthony-Twarog & Twarog (1987), and Anthony-Twarog et al. (1988) (AT87/88) are also shown.

(Nissen 1988) to $(m - M)_0 = 9.83$ (Anthony-Twarog & Twarog 1987), reddening and metal abundance of $E_{(b-y)} = 0.076 \pm 0.012$ and $[Fe/H] = 0.18 \pm 0.05$ (Nissen 1988), and age from 1.3 *Gyr* (Mazzei & Pigatto 1988) to 2.4 *Gyr* (Anthony-Twarog et al. 1988).

3. Observations and data reduction

Photometric observations of IC 4651 in the Strömrgren *uvby* system were made during May 1–3, 1997 using the Danish 1.54m telescope and DFOSC focal reducer (J. Andersen et al. 1995) at ESO, La Silla, Chile, equipped with a Loral $2 \times 2K$ CCD at a scale of $0''.39/\text{pixel}$. The observations cover a field with a radius of $\sim 11'$, roughly centered on the cluster (Fig. 1). Image diameters (FWHM), including all contributions from the optics and CCD, were $1''.25 - 1''.9$ on the first night, $1''.5 - 2''.0$ the second night, and $1''.1 - 2''.0$ the third night. The first and second night were photometric, the third was not (see Sect. 4.1). A total of 89 frames were obtained, evenly distributed among the four filters.

To eliminate systematic effects from the CCD, such as gradients in quantum efficiency and/or bad columns, rows or single pixels, exposures were made in three different position angles: ($-90^\circ, 0^\circ$ and $+90^\circ$) and subsequently averaged (Andersen et al. 1995).

Individual pointings were systematically offset with respect to the reference frame, which was centered roughly on the cluster. Nine offsets spanning from $-5'$ to $+5'$ in right ascension

(α) and declination (δ) were used. For each of the nine offsets, at least two exposures in each filter were acquired. Table 1 (Available in electronic form only) contains information about the Date, Night, Filter, Exposure time, Airmass, CCD rotation angle, and α, δ -offsets for all 89 frames.

A total of 69 bias frames and 16 30-minute dark exposures were also taken, evenly distributed over the observing run. In addition, 67 sky flat-fields (SFF) were obtained during the evening and morning twilight, 25 in *u* and 14 in each of *b, v* and *y*.

3.1. Basic reductions

All science frames were bias corrected by subtraction of a *master bias*, computed by combining all bias frames. The bias level increased slightly during the period of observation, possibly due to a slow contamination from cabling inside the dewar (a problem found and removed in January 1998). Because of this variation, subtraction of the *master bias* could not completely remove the electronic background from the individual science frames. A median value for the signal in the overscan region of each frame was therefore also subtracted.

Analysis of the dark frames proved that the dark signal was insignificant.

For each filter (*u, v, b* and *y*), a *master-SFF* was created by combination of the best single SFF's. In order to reduce the effects of gradients in the quantum efficiency of the chip, overall gradients in the twilight sky, and scattered light in the telescope and instrument, the CCD was rotated 180° between each pair off SFF exposure (Andersen et al. 1995).

3.2. Point-Spread Function (PSF) photometry

PSF photometry was carried out for the stars in this moderately crowded field (1500–10000 stars per frame, depending on filter and exposure time), using the DAOPHOT software (Stetson 1987; Stetson 1989c). In each frame, 50 bright stars were used to derive a point-spread function, which was allowed to vary quadratically with position. Because of vignetting from the round filters, it was necessary to eliminate detections in the four corners and at the edges of the images. Coordinate transformations were set up (Stetson 1989a) to refer positions on each CCD frame to the coordinate system of the reference frame (centered on the cluster). The methods of synthetic aperture photometry and growth-curve analysis (Stetson 1990) were used in order to obtain the relative calibration of the images.

4. Standard stars

In order to increase the number of photoelectric standard stars available for the transformations to the *uvby* standard system above those in IC 4651 itself (Nissen 1988), the open cluster M67 (Nissen et al. 1987) and a number of isolated standard stars were also observed. These standard star observations were made each night before and after the observations of IC 4651.

The CCD images obtained in this study reveal that three of the 10 stars by Nissen (1988) have close companions within

the diaphragm, bright enough to cause magnitude errors larger than 0^m01 . Hence, these were excluded as standard stars. For the same reason, 12 stars out of the 64 stars in the central region of M67 with photoelectric *uvby-H_β* photometry (Nissen et al. 1987) were excluded. The remaining standard stars in IC 4651 (7 stars) and in M67 (52 stars) were used in this study.

In addition to the stars in IC 4651 itself and in M67, 19 bright isolated secondary standard stars from Olsen (1983, 1984) and Schuster & Nissen (1988) were observed each night before and after the program observations. This was done to increase the color range of the standard transformations: A large color range ($(b - y) = 0.05\text{--}0.6$) improves the least-squares determination of the transformation coefficients (Stetson1989b) and permits reliable photometry of stars in both the turnoff and main-sequence region.

The magnitudes of the isolated standard stars were determined from the convergence of their growth-curves. Only stars with well defined growth-curves, i.e. a magnitude error below 0^m01 , were accepted. Magnitudes were determined in *y* for 27 stars, in *b* for 18 stars, in *v* for 18 stars, and in *u* for 20 stars.

4.1. Transformation to standard system

The differences between standard and observed magnitudes ($m_{std} - m_{obs}$) for all standard stars were plotted against all parameters which could possibly be correlated with the residuals. The quantities tested were: the color indices $(v - y)$, $(u - y)$, and $(b - y)$, the Strömgren Balmer discontinuity index c_1 and metallicity index m_1 , the Universal Time (*UT*) for the exposure, the exposure time (*expt*), the azimuth angle (*az*), the stellar magnitude (*m*), and the airmass (*X*). Tests for dependence of the residual on each of these parameters were carried out for the standard star observations in each filter *u*, *v*, *b* and *y* and for each night. This examination led to transformation equations including terms in airmass (*X*) and $(v - y)$ only.

The transformation coefficients were derived by simultaneous linear least squares fitting (Stetson1989b) to the $(m_{std} - m_{obs})$ vs. *X*, $(v - y)$ dataset. The following transformation equations were obtained for night 1 (extinction coefficients for night 2 given in parentheses):

$$V_{std} = y_{obs} - (2.930 + 0.135(0.132)X + 0.001(v - y)_{std})$$

$$b_{std} = b_{obs} - (2.853 + 0.196(0.201)X + 0.040(v - y)_{std})$$

$$v_{std} = v_{obs} - (2.889 + 0.282(0.295)X + 0.061(v - y)_{std})$$

$$u_{std} = u_{obs} - (2.772 + 0.513(0.534)X + 0.059(v - y)_{std})$$

The transformation coefficients for night 3 deviated considerably from those from night 1 and 2. Suspicion of non-photometric conditions therefore led to the temporary exclusion of the data from night 3. After transformation of the data from night 1 and 2 to the standard system, the data from night 3 were transformed to the night 1 and 2 standard data.

Comparing the standard data by Nissen with the transformed data of the present study for the 7 standard stars in IC 4651 (Nissen 1988) and for the 49 standard stars in M67 (Nissen et al. 1987) gives a mean difference in *V* of $0^m0063 \pm 0.0111$

(s.d.) and $0^m0020 \pm 0.0170$ (s.d.), respectively, and a mean difference in $(b - y)$ of $-0^m0044 \pm 0.0093$ and $-0^m0003 \pm 0.0151$, respectively, with no significant dependence on color and magnitude.

4.2. Photometric precision and accuracy

The final magnitude of a star is determined as the *weighted mean* of the individual detections. The number of detections of each star depends on its location and brightness. The maximum number of measurements of a single star in a single filter is 18.

The precision measured as the standard deviation (s.d.) of one instrumental magnitude, calculated for stars observed more than 5 times in each of the four filters, is: 0^m01 in *V*, 0^m01 in *b*, 0^m015 in *v* and 0^m02 in *u*.

After transformation to the standard system, the accuracy in terms of *standard error of the weighted mean* (sewm) (Stetson1989b), for stars detected more than 5 times, converge at approximately: 0^m007 for *V*, 0^m007 for *b*, 0^m009 for *v*, and 0^m01 for *u* for the brightest stars.

Standard deviations of the residuals $m_{std}(calculated) - m_{std}(catalog)$ were calculated for all standard stars. For the isolated standard stars the s.d. ranges from 0^m0318 in *V* on night 1 to 0^m0056 in *V* on night 2. For standard stars in M67, s.d. range from 0^m015 in *V* on night 2 to 0^m0364 in *u* on night 2. The s.d. for the standards in IC 4651 range from 0^m011 in *b* on night 1 to 0^m019 in *u* on night 1.

4.3. Comparison with previous photometric studies

Fig. 2 shows the differences in *V* and $(b - y)$ between Anthony-Twarog and Twarog (1987) and this study for about 60 stars in IC 4651. The solid lines indicate the mean difference: $0^m0048 \pm 0.0324$ (s.d.) for all stars in *V* and $0^m0029 \pm 0.0096$ (s.d.) for 45 stars in $(b - y)$. Data for the red giants, $V < 11^m$ or $(b - y) > 0.6$ (dotted vertical line in lower panel) are less reliable because the color-range of the standard stars does not extend beyond this limit. The dotted horizontal line in Fig. 2 (lower panel) denotes the upper limit (0.03) for color differences included in the calculation of the mean.

5. Star numbering conventions

Five different numbering systems have been in use for stars in IC 4651: Eggen 1971 (prefix E), Lindoff 1972 (prefix L), Anthony-Twarog & Twarog 1987, Anthony-Twarog et al. 1988, and Piatti et al. 1998. Eggen's numbering has been used most frequently in discussions of the red giants and turn-off stars. Anthony-Twarog et al. identified primarily fainter stars and give cross-references to Eggen; no cross-references are given by Piatti et al. 1998.

There are good reasons for introducing a new numbering system for IC 4651: 1) the present photometry covers a much larger field and includes more (~ 17000) and considerably fainter stars than previous studies, 2) essentially all stars measured in any previous study are included in the present photom-

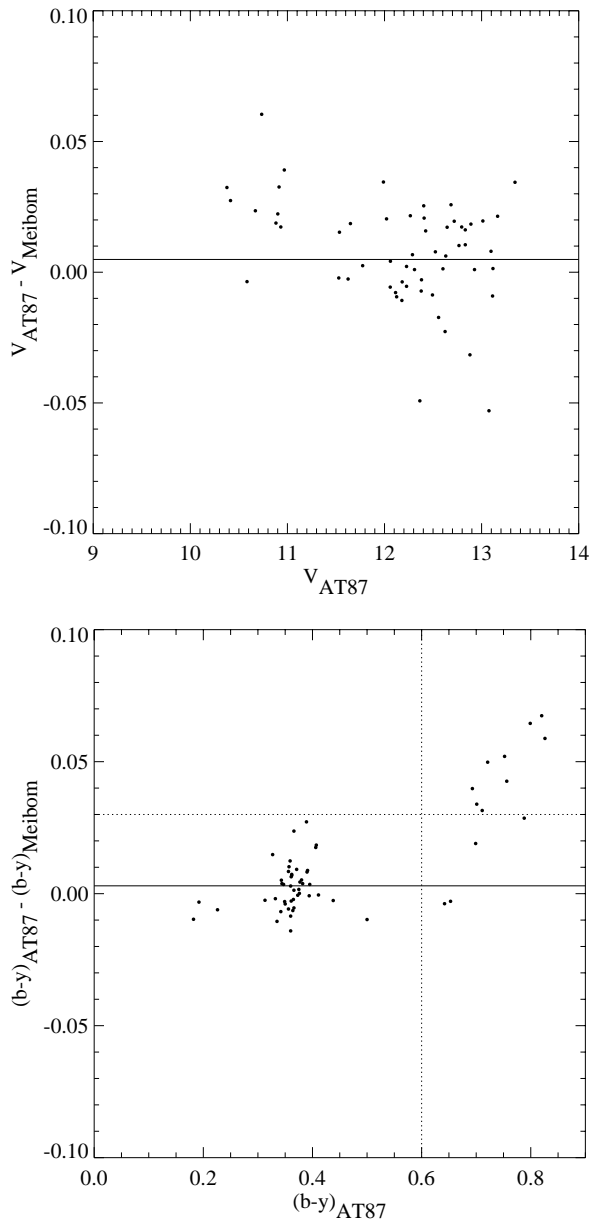


Fig. 2. Difference in V (upper panel) and $(b-y)$ (lower panel) between Anthony-Twarog and Twarog 1987 and the present study for about 60 stars in IC 4651. The mean differences are indicated by the solid lines. Dotted lines indicate the upper limit in color-range for standard stars (vertical) and the upper limit for color $(b-y)$ differences (horizontal) included in the mean; stars above these limits are red giant stars.

etry, and 3) a large number of cluster stars, both bright and faint, are found outside the fields studied previously (see below).

The new numbering system uses prefix MEI, and the stars are ordered by right ascension and numbered from 1 to 17640. Table 2 (Available in electronic form only) gives cross-references between the MEI-system and the Lindoff (1972), Eggen (1971), Anthony-Twarog & Twarog (1987), and Anthony-Twarog et al. (1988) identification numbers.

Accurate coordinates are more precise guides to stellar identifications than labeled finding charts or raw pixel coordinates

(X, Y) . Accordingly, J2000 coordinates for all stars measured on all CCD frames have been determined using numerous reference stars from the Digitized Sky Survey. The resulting accuracy is better than $1''$ in both coordinates. Table 3 (Available in electronic form only) is the final catalogue of the new photometry, ordered by MEI identification number. For each star, it gives the MEI number, J2000 coordinates, the new y , b , v , and u magnitudes in the standard system, and their mean errors.

6. The color-magnitude diagram

The color-magnitude diagrams (CMD) on the standard system are presented in Figs. 3 and 4 which show $(b-y)$ vs. V and $(v-y)$ vs. V , respectively. All stars measured in the field of IC 4651 are included. When comparing with previous studies, it is noted that:

First, there is a large increase in the number of stars in the CMD due to the much larger field and fainter limiting magnitude.

Second, the “new” stars more than double the number of probable member stars in the turnoff region (unpublished radial-velocity data by Nordström & Andersen show that field star contamination in this region of the CMD is small).

Third, two previously unknown giant candidates have been added to the sixteen red giants already known.

Fourth, the area on the sky covered by cluster stars is approximately doubled: IC 4651 is much larger and richer than suspected in any previous studies.

Fifth, a previously undetected sequence of faint cluster main-sequence stars (Fig. 4), extremely tightly defined in the $(v-y)$ vs. V diagram (less clearly so in the $(b-y)$ vs. V CMD) is visible down to approximately $V \sim 18^m$. This greatly increases the value of IC 4651 as a diagnostic of stellar evolution models and as a probe of the dynamical evolution of star clusters. A similar faint main-sequence was absent in the “sister” cluster NGC 3680, which has the same age and turn-off mass and a comparable number of red giants (Nordström et al. 1997).

6.1. The red giant region

The dominant feature of the red giant branch is the clump of stars in the brightness range of $10^m5 - 11^m0$ in V , and $0.65-0.72$ in $(b-y)$. In addition to the 10 stars making up the red giant clump itself, six other red giant stars are scattered around it (Mermilliod et al. 1995). Two “new” stars (MEI4353 and MEI11218) are found in the red giant region of the CMD. The colors of the red giants in IC 4651 are not covered by the color range of the standard stars used in the standard transformations. Therefore, precise comparison of the colors and magnitudes for the cluster giants with earlier studies or with stellar models cannot be made.

6.2. The turn-off region

Figs. 3 and 4 show that the cluster sequence begins to evolve away from the zero-age main-sequence (ZAMS) at $V \simeq 14^m5$; the tip of the turn-off is at $V \simeq 12^m$. About 160 newly dis-

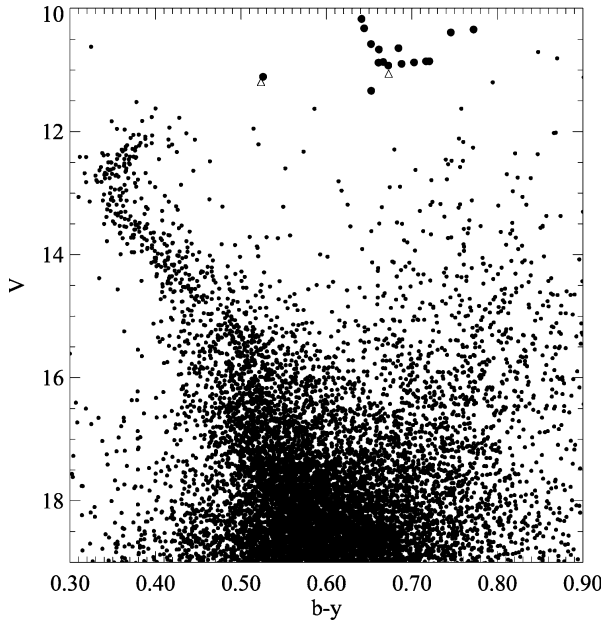


Fig. 3. The final $(b-y)$ vs. V CMD of IC 4651. Large solid dots denote stars in the red giant region, triangles “new” red giant candidates.

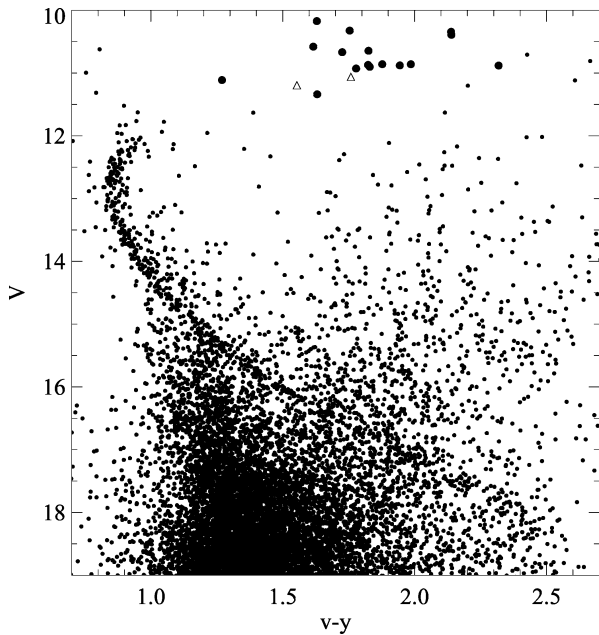


Fig. 4. The final $(v-y)$ vs. V CMD of IC 4651. Large solid dots denote stars in the red giant region, triangles “new” red giant candidates.

covered stars from regions of the field outside those covered by earlier photometric studies appear in this magnitude range, more than doubling the known population of turn-off stars in IC 4651.

6.3. The lower main-sequence and the distance to IC 4651

In the $(v-y)$ vs. V CMD (Fig. 4) the main-sequence is clearly defined down to $\sim 18^m$. This result contradicts the assertion of Anthony-Twarog & Twarog (1987) and Anthony-Twarog et al.

(1988) that the main-sequence of IC 4651 is poorly defined or totally missing below $V \simeq 14^m5$. The probable cause of the earlier result is discussed in Sect. 6.5 below.

Numerous determinations of the distance to IC 4651 exist, ranging from $(m-M)_0 = 9.40$ to $(m-M)_0 = 9.83$ (Kjeldsen & Frandsen 1991, and references therein). Previous attempts, e.g. (Anthony-Twarog et al. 1988; Bertelli et al. 1992), relied on fitting theoretical isochrones to a broad average sequence of main-sequence and turn-off stars, introducing uncertainties from both color transformations and bolometric corrections as well as in the definition of the main-sequence itself.

Using the Hyades for a direct distance determination has several advantages: The Hyades are stars with precisely known distances, the same metallicity as IC4651 (Nissen 1988), and also cover the same colour range as the stars of IC 4651. The well defined deep main-sequence in IC 4651 resulting from the present photometric study enables fitting of the Hyades main-sequence over a large range in colour, and thus provides a means for accurate determination of the distance to the cluster. The distance modulus for the Hyades (Perryman et al. 1998), using absolute trigonometric parallaxes from the Hipparcos catalogue, is $(m-M)_0 = 3.33 \pm 0.01$ corresponding to a distance of 46.34 ± 0.27 pc. The Hyades main-sequence (M_V , $(B-V)$) used in this study is that by Schwan (1991), who found a distance modulus of $(m-M)_0 = 3.40 \pm 0.04$, but correcting the absolute magnitudes to the new HIPPARCOS zero-point. The main-sequence relation was transformed to the Strömgren system via a plot of $(B-V)$ vs. $(b-y)$ indices for stars observed by Crawford & Perry (1966) and Olsen (1993). $(v-y)$ indices were obtained by internal transformation in the Hyades, using the observed four colour Strömgren photometry from the same sources.

Fig. 5 shows the Hyades main-sequence fitted to the cluster main-sequence, using the best-fit true distance modulus of $(m-M)_0 = 10.03$, which is adopted as the distance modulus of IC 4651 in this study. The uncertainty on the distance modulus is estimated to 0^m1 on the basis of the scatter around the Hyades main-sequence in the CMD. The resulting distance to IC 4651 is then 1.014 ± 0.05 kpc.

6.4. Why is the $(v-y) - V$ CMD so superior?

Figs. 4 and 3 show that the cluster sequence is much better defined in the $(v-y) - V$ CMD compared to the $(b-y) - V$ diagram, which is the closest approximation to the conventional $(B-V) - V$ CMD. Especially evident is the better contrast of the cluster lower main-sequence from the field star population. As a guide to the choice of color bands in future studies of cluster CMDs, one would like to understand why this is so.

The scatter of the cluster sequence does increase from $(b-y)$ to $(v-y)$ in absolute terms, as expected from the computed photometric uncertainties. However, relative to the color range spanned by the main-sequence from the turnoff to, say, $V = 18$, the influence of photometric errors in color is clearly smaller in $(v-y)$ than in $(b-y)$. This explains part of the superior performance of the $(v-y) - V$ CMD.

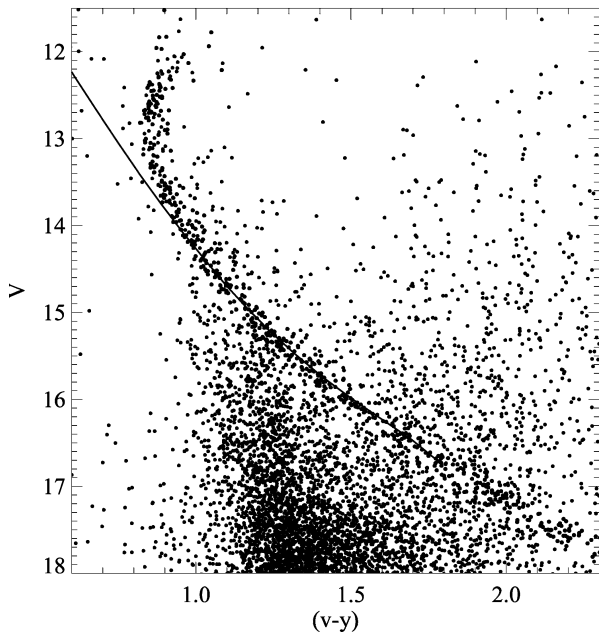


Fig. 5. The Hyades main-sequence fit to that of IC 4651 for a distance modulus of 10.03. The long stretch of the lower main-sequence which is available for the fit in the $(v-y)$ vs. V CMD (to $V \sim 18^m$) enables a very accurate determination.

An additional explanation could be different influence of interstellar reddening. Using the reddening relations of Crawford & Mandwewala (1976), one can compute the direction of the reddening vectors in all three CMDs: V vs. $(b-y)$, $(v-y)$, and $(u-y)$. The reddening vectors become less steep along this sequence, because the reddening corresponding to a fixed amount of extinction in V increases. However, as illustrated in Fig. 6, the slope of the lower main-sequence decreases even more rapidly. As a result, the strong concentration of distant field stars below and to the blue of the cluster main-sequence will be scattered *across* the cluster sequence in the $(b-y)$ diagram, but roughly *parallel* to the cluster sequence in the $(v-y)$ CMD. Thus, differences in reddening of the background field stars will tend to smear the field and cluster distributions more in a $(b-y)$ CMD than in a $(v-y)$ CMD.

This result can be useful in clusters with differential reddening too: The right combinations of color bands will enable determination of CMDs in which the effects of differential reddening would be either minimized or maximized. Minimizing the effect of differential reddening will ease the study of the cluster sequence itself, while alternatively maximization of the effect of differential reddening will help estimate the amount of reddening for individual cluster stars and hence help to map the distribution of reddening over the cluster.

6.5. Radial variations in the CMD

Fig. 7a-d show separate CMD's for stars in different radius intervals from the center of IC 4651. Changes in the CMD with radial distance (R) from the center are apparent: a) $R < 4.7'$.

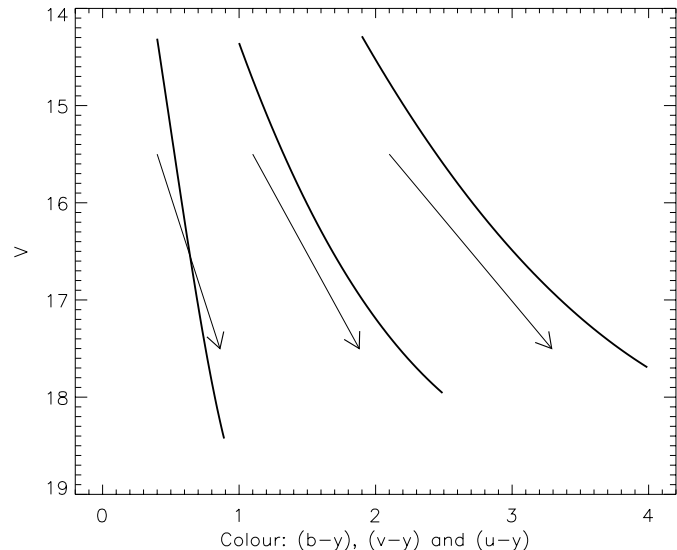


Fig. 6. Plot of the reddening vectors and lower main-sequences (shown as fitted polynomial curves for clarity) for each of the three color indices $(b-y)$, $(v-y)$, and $(u-y)$.

The turn-off region is well defined, but the lower main-sequence is poorly defined. b) $4.7' < R < 7.1'$. The turn-off region is still well defined, but less than in a), while the lower main-sequence is slightly better defined than in a). c) $R > 7.1'$. The turn-off region is relatively poorly defined while the lower main-sequence is clearly defined and reaches fainter magnitudes than in a) and b). d) $0 < R < 12'$. The full sample. Both turn-off and main-sequence regions are well defined.

While the field covered in Fig. 7c is significantly larger than the fields covered in Fig. 7a and b, there does appear to be a correlation between radial distance from the center and the CMD of IC 4651. The ratio of upper to lower main-sequence stars is decreasing away from the center. This is indeed the expected result of the dynamical evolution and mass segregation in the outer part of the cluster.

Anthony-Twarog et al. (1988) compared the density of faint stars ($V \gtrsim 14^m.5$) from their central cluster field ($R \lesssim 5'$) with the density of stars at similar magnitudes in a photographically measured semi-annulus between $R = 4.7'$ and $R = 7.1'$. Assuming that the outer annulus represented the general field beyond the limit of the cluster itself, and finding that the densities of stars in the two areas were quite similar, they concluded that there was no significant population of cluster stars at those magnitudes.

However, the present study reveals the presence of numerous cluster stars also in the annulus $4.7' < R < 7.1'$. This area is thus not a clean sample of the background sky. On the contrary, dynamical evolution appears to have preferentially driven the fainter, less massive main-sequence stars from the central regions out into just this annulus, creating a lack of contrast between the central and outer fields which was interpreted as an actual lack of faint stars.

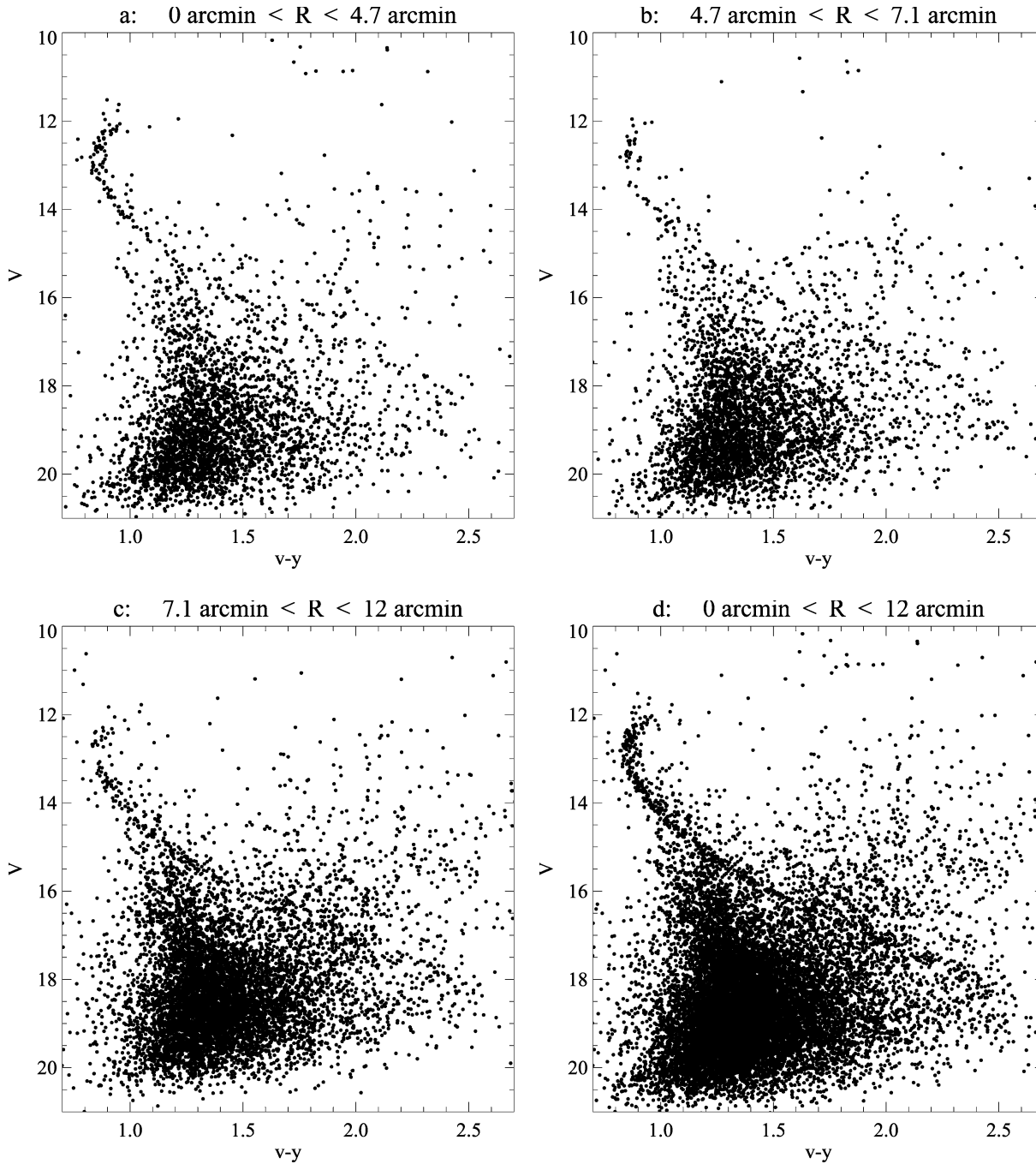


Fig. 7. **a–c:** CMDs for samples of stars with increasing radial distances from the center of IC 4651. **d:** CMD from all stars detected in the new field on IC 4651.

7. Conclusions

The new, deep Strömgen *uvby* photometry of stars in a large field centered on IC 4651 has profoundly changed the traditional understanding of this cluster. The main results can be summarized as follows:

1. A catalogue of accurate *uvby* photometry and J2000 coordinates for 17,640 stars in a field of approx. $11'$ radius centered on IC 4651. Given the larger area coverage and greater depth
2. These data show IC 4651 to be at least twice as large in area and much richer in stars than previously believed. Many cluster stars, both bright and faint, are found outside the cluster regions surveyed in previous studies.
3. A previously undetected lower cluster main-sequence is clearly delineated down to $V \simeq 18$. This has made accurate determination of the distance to IC 4651 (1.014 ± 0.05 kpc)

of the new photometry, a new numbering system for stars in this field is introduced.

possible by a direct fit to the Hyades main-sequence, and enables fits of theoretical isochrones with far greater accuracy than previously obtained for IC 4651.

4. The CMD based on the color index $v - y$ is found to provide much superior definition of the lower main-sequence, including better separation of cluster and field stars. This is due to the reduced effect of photometric errors and, more importantly, a reddening vector that is parallel to the cluster sequence rather than intersecting it. This technique should have interesting applications to clusters with differential reddening.
5. The CMD as a function of radial distance from the center of IC 4651 shows preliminary, but clear indications of dynamical evolution and mass segregation in the cluster, with a large fraction of faint main-sequence stars found outside the cluster region covered in previous studies.

A closer analysis of membership and the stellar and dynamical evolution of IC 4651, based on the present data and additional radial-velocity information (J. Andersen and B. Nordström, priv. comm., 1998), will be the subject of a forthcoming paper.

Acknowledgements. I am grateful to Johannes Andersen and Birgitta Nordström for their enthusiastic and highly instructive support during this work. Likewise, I am grateful to Frank Grundahl for help, supervision, and encouragement through the whole process (observations, data reduction/photometry, and data analysis), and to Michael I. Andersen for his important help in planning the observations and performing the data reductions and photometry. Observing with the Danish 1.5 m telescope at La Silla, Chile, was highly motivating, thanks to the colleagues mentioned and to the travel support received from the Danish Natural Science Research Council via The Danish Astronomical Instrument Center. I thank Robert Mathieu for comments on the manuscript, discussion, and support under National Science Foundation grant AST 9731302. I also thank Keivan Stassun for help with the astrometric solutions, and the Digitized Sky Survey (DSS) for providing the required astrometric reference data.

References

- Andersen J., Andersen M.I., Klougart J., et al., 1995 ESO Messenger 79, 12
- Andersen M.I., Freyhammer L.M., Storm J., 1995 In: Benvenuti P. (ed.) Understanding and Calibrating HST and ESO Instruments
- Andersen J., Nordström B., 1998, (Private communication)
- Anthony-Twarog B.J., Twarog B.A., 1987, AJ 94, 1222
- Anthony-Twarog B.J., Mukherjee K., Caldwell N., Twarog B.A., 1988, AJ 95, 1453
- Bertelli G., Bressan A., Chiosi C., 1992, ApJ 392, 522
- Carraro G., Bertelli G., Bressan A., Chiosi C., 1993, A&AS 101, 381
- Crawford D.L., Mandwewala N., 1976, PASP 88, 917
- Crawford D.L., Perry C.L., 1966, AJ 71, 206
- de la Fuente Marcos R., 1997, A&A 322, 764
- Demarque P., Sarajedini A., Guo X.-J., 1994, ApJ 426, 165
- Eggen O.J., 1971, ApJ 166, 87
- Eggen O.J., 1989, PASP 101, 366
- Friel E.D., 1995, ARA&A 33, 381
- Gilmore G., King I.R., and van der Kruit P.C., 1990, The Milky Way as a Galaxy. University Science Books
- Kjeldsen H., Frandsen S., 1991, A&AS 87, 119
- Lindoff U., 1972, A&AS 7, 231
- Mazzei P., Pigatto L., 1988, A&A 193, 148
- Mermilliod J.C., Andersen J., Nordström B., Mayor M., 1995, A&A 299, 53
- Meynet G., Mermilliod J.C., Maeder A., 1993, A&A 98, 477
- Nissen P.E., Twarog B.A., Crawford D.L., 1987, AJ 93, 634
- Nissen P.E., 1988, A&A 199, 146
- Nordström B., Andersen J., Andersen M.I., 1997, A&A 322, 460
- Olsen E.H., 1983, A&AS 54, 55
- Olsen E.H., 1984, A&AS 57, 443
- Olsen E.H., 1993, A&AS 102, 89
- Perryman M.A.C., Brown A.G.A., Lebreton Y., et al., 1998, A&A 331, 81
- Piatti A.E., Claria J.J., Bica E., 1998, ApJS 116, 263
- Schuster W.J., Nissen P.E., 1988, A&AS 73, 225
- Smith G.H., 1982, AJ 87, 360
- Spitzer L., Mathieu R.D., 1980, ApJ 241, 618
- Stetson P.B., 1987, PASP 99, 191
- Stetson P.B., 1989a, priv. comm., Dominion Astrophysical Observatory, Victoria, Canada, Notes (manual-style)
- Stetson P.B., 1989b, The Technique of Least Squares and Stellar Photometry with CCD's. Dominion Astrophysical Observatory, Victoria, Canada, Lecture Notes
- Stetson P.B., 1989c, User's Manual for DAOPHOT II, Dominion Astrophysical Observatory, Victoria, Canada
- Stetson P.B., 1990, PASP 102, 932
- Schwan H., 1991, A&A 243, 386
- VandenBerg D.A., 1983, ApJ 51, 29
- VandenBerg D.A., 1985, ApJ 58, 711